

Available online at www.sciencedirect.com**ScienceDirect**

Energy Procedia 49 (2014) 1491 – 1500

Energy

Procedia

SolarPACES 2013

Comparison of linear and point focus collectors in solar power plants

F.Rinaldi^a, M.Binotti^{a*}, A.Giostrì^a, G.Manzolini^a^a Politecnico di Milano, Dipartimento di Energia, Via Lambruschini 4, 20156 Milano, Italy

Abstract

Solar tower based plants are seen as a promising technology to reduce the cost of electricity from solar radiation. This paper assesses the design and overall yearly performances of two different solar tower concepts featuring two commercial plants running in Spain. The first plant investigated is based on Direct Steam Generation and a cavity receiver (PS-10 type). The second plant considers an external cylindrical receiver with molten salts as heat transfer fluid and storage system (Gemastar type). About the optical assessment performed with DELSOL3, a calibration of heliostat aim points was performed to match available flux maps on the receiver. Moving to results, the PS-10 type has higher optical performances both nominal design and yearly average. This is due both to the field size and orientation which guarantee a higher efficiency and to the receiver concept itself. About power production, the molten salts allow higher temperature and consequently conversion efficiency than PS-10. The solar-to-electricity efficiency is equal to 18.7% vs. 16.4% of DSG cavity plant. The obtained results are strictly related to the set of assumptions made on each plant component: when available real plant data were used. The two solar tower plants results were also compared to corresponding commercial linear focus plants featuring the same power block concept. Gemastar type shows a higher solar-to-electricity efficiency compared to a parabolic trough plant with storage (18.7% vs. 15.4%) because of the higher maximum temperatures and, consequently, power block efficiency. PS-10 is better than a linear Fresnel DSG (16.4% vs. 10.4%) because of the higher optical performances.

© 2013 The Authors. Published by Elsevier Ltd. This is an open access article under the CC BY-NC-ND license

(<http://creativecommons.org/licenses/by-nc-nd/3.0/>).

Selection and peer review by the scientific conference committee of SolarPACES 2013 under responsibility of PSE AG.

Final manuscript published as received without editorial corrections.

Keywords: Solar Tower, Heliostat field, Solar thermal plants simulation.

* Corresponding author. Tel.: +39-02-2399-3935; fax: +39-02-2399-3913.

E-mail address: marco.binotti@polimi.it

1. Introduction

Solar thermal power plants can give a fundamental contribution to the reduction of CO₂ emissions, air pollutants as well as fossil fuels consumption. Parabolic Trough (PT) collectors have been the reference technology in the last thirtyish years since the first SEGS plant was built in 1985, but in recent years both Linear Fresnel Reflectors (LFR) and Power Tower technologies are gaining the attention of the scientific community as well as of the electric companies. LFR are expected to bring the plant costs down thanks to the simpler concept, while Power Tower technologies has potential better yearly performances than PT thanks to their usually higher maximum temperatures that improve power cycle efficiency. For the same reason, power tower concept can be extended also to fuel production [1].

In the present publication, the yearly performances of two power tower plants in operation are assessed: the first plant is a Gemasolar type [2], while the second one is a PS-10 type plant [3].

The Gemasolar plant, in operation since 2011, is a 20 MWe1 power plant located near Sevilla (SP) using molten salts as HTF and implementing a 15 hours direct thermal storage system. The solar field is based on the surrounded field concept with 2650 heliostats, 110 m² wide each. The thermal power recovered into the tower is converted in electricity with a conventional Rankine cycle with steam superheating (SH) and a reheating (RH).

The second considered plant is based on a direct steam generation technology, with saturated steam, featuring the PS-10 plant in Sevilla which is in operation since 2007. The net power output is of 11 MWe1 and the power section includes a small direct steam storage of about 25 min. The solar field has the north configuration counting 624 heliostats. The 40 bar saturated steam produced in the tower is directly expanded in the power cycle steam turbine. The performances of Gemasolar and PS-10 were assessed both at design and annual conditions. Calculated results were then compared with two CSP commercial reference cases based on linear collectors. Gemasolar is compared to a Parabolic Trough plant with thermal energy storage (i.e. Andasol 1 type plant), while PS-10 with a direct steam generation plant based on LFR technology (i.e. Puerto Errado 1 type plant). Reference case nominal and yearly performances were calculated with the same simulation tool (Thermoflex 23[®] [4]) used in this work for the two solar tower cases. In order to make a consistent comparison, all calculation are performed assuming Sevilla's geographical coordinates (37°42' N, 5° 9' W) and annual Direct Normal Irradiance (2090 kWh/m²/y).

The aim of this work is to compare the performances of real plants, accepting different operating conditions and components characteristics. The authors do not want to suggest any configurations as the best one, also because the parameter to be used is the cost of electricity.

2. Methodology

The on-design and yearly performances of the two solar plants are modeled using two different tools: DELSOL3 [5] and Thermoflex 23[®] [4]. DELSOL3 was used to assess the optical efficiency and the Incidence Angle Modifier (IAM) maps for the two investigated solar tower plants. The optical performances were then used as input for the overall plant assessment performed with the commercial software Thermoflex 23[®]. A VBA suite was written in order to include proper plant management strategies.

The plant performances are evaluated both at design and average yearly conditions. Because of the different size of the investigated plants as well as the reference cases, the comparison will be performed in terms of efficiency. In order to outline the conversion process losses, the solar-to-electric efficiency is calculated as product of each conversion step as expressed in eq.(1) (this methodology was already adopted in previous works [6] [7] [8]):

$$\eta_{overall} = \eta_{optical} \cdot \eta_{thermal} \cdot \eta_{piping} \cdot \eta_{net_PB} \cdot \eta_{aux_SF} = \frac{E_{el,annual}}{E_{SUN}} \quad (1)$$

where:

- $\eta_{optical}$ is the optical efficiency that compares the radiation absorbed by the receiver to the direct normal solar irradiation;
- $\eta_{thermal}$ is the thermal efficiency that takes into account the receiver thermal losses;
- η_{piping} evaluates the impact of piping thermal losses (also nighttime losses) on the HTF transferred thermal power
- η_{net_PB} expresses the efficiency conversion of the thermal input into electricity;

- η_{aux_SF} expresses the impact of solar field circulating pumps and tracking consumptions on the net power block output.

At nominal conditions, all terms in Eq. (1) are evaluated on the basis of power (Watts), whereas in the annual assessment on the basis of energy (Joules) estimated over 8,760 hours with an hourly time frame.

3. Optical assessment

The optical performances of the two considered plants were obtained with DELSOL3, a performance and design code developed at the SANDIA NATIONAL LABORATORIES for optical and economic analyses [5]. The program requires as input the solar plant geographical coordinates, the atmospheric conditions (DNI, atmospheric attenuation, etc.) the geometrical description of the heliostats as well as their optical characterization; the user can select the receiver type between three different receiver options (external, flat plate and cavity receiver) and each shape can be characterized through proper geometrical specifications. Different aiming strategies can also be used. The optical performance of the heliostat field can be computed either in a given time of the year or for a combination of different Azimuth and Zenith angles, in order to calculate the IAM (Incidence Angle Modifier) map. The program gives as output the solar field optical efficiency (η_{opt}) split into six components:

- η_{cos} is the solar radiation reduction, proportional to the cosine of the angle between the sun rays and the heliostat surface normal;
- $\eta_{reflect}$ is the average mirror reflectivity;
- η_{shadow} is related to the shading losses, due to the shadow cast by a mirror onto the mirrors behind it and takes into account the receiver tower shadow on the whole solar field
- η_{block} is related to the blocking losses, due to the radiation reflected by a heliostat on the back of another heliostat;
- $\eta_{attenuation}$ takes into account the atmospheric attenuation of the radiation between the heliostat and the receiver;
- $\eta_{spillage}$ represents the fraction of the energy spot reflected that hits onto the receiver surface.

The optical efficiency can thus be obtained as the product of the six abovementioned efficiencies according to:

$$\eta_{optical-DELSOL3} = \eta_{cos} \cdot \eta_{reflect} \cdot \eta_{shadow} \cdot \eta_{block} \cdot \eta_{attenuation} \cdot \eta_{spillage} \quad (2)$$

This efficiency does not take into account the receiver absorbance. An Excel spreadsheet was used to fasten input and output handling and to post-process the obtained results.

The PS10 and Gemasolar solar field optical models were created in DELSOL3, through Excel[®], according to data available in literature [2] [9] [10] [11]; the DELSOL3 code was modified in order to increase the maximum allowable number of heliostats per row, as required in the modeling of the Gemasolar solar field. The position of each heliostat for the two fields was taken from aerial views of the plants; every heliostat was assumed spherically curved, with a focal point equal to the slant range to the receiver [3]; the optical errors were taken equal in the two investigated lay-out. The mirror reflectivity of the PS10 heliostats was assumed equal to 88% as reported in [10].

Table 1. PS10 and Gemasolar heliostat fields main geometrical and optical assumptions.

	PS10	Gemasolar
Number of heliostats in the field	624	2650
Field shape	North	Surrounded
Heliostat width (m)	12.84	11
Heliostat height (m)	9.45	10
Curvature	Spherical	Spherical
Reflectivity	0.88	0.93
Reflective/Total area ratio	1	1
Total Error on Reflected ray (mrad)	2.9	2.9
Focus	Slant Range	Slant Range

Information on the Gemasolar heliostats cleaning shows a reflectivity value in the range 90-96% [9]: therefore, an average value of 93% was assumed. The main geometrical and optical assumptions for the two heliostat fields are summarized in Table 1. The atmospheric attenuation for the two solar fields was computed in DELSOL3 as a function of each heliostat slant range (DELSOL3 option 'ATM = 0' for clear sky condition) according to the following equation [5]:

$$(100 - \eta_{\text{attenuation}}) = 0.6739 + 10.46R - 1.70R^2 + 0.2845R^3 \quad (3)$$

where R is the slant range of each mirror in km.

The calculations were performed with the conservative assumption of no overlap between blocking and shading effects. Besides the heliostat field configuration, the two investigated plants differ also for the tower concept: the PS10 has a cavity receiver composed by four panels placed at semicircle behind a rectangular aperture, while the Gemasolar tower uses an external cylindrical receiver. Main geometrical assumptions are reported in Table 2.

Table 2. PS10 and Gemasolar receiver geometrical assumptions used as input in DELSOL3.

	PS10	Gemasolar
Receiver elevation (m)	93.2	116
Tower height (m)	107.7	134
Tower diameter (m)	18	8
R (m)	7	-
W (m)	4	-
Aperture height (m)	16	-
Aperture width (m)	14.83	-
Panel height (m)	12	-
Single panel width (m)	5.36	-
Receiver height (m)	-	16
Receiver diameter (m)	-	8

Receiver elevation and tower height are relative to the heliostat pivot point, not to the ground level. The shadow cast by the tower is taken into account assuming it as a cylinder, defined by *tower height* and *tower diameter*. As in DELSOL3 the performance calculation refers to the radiation that reaches the aperture, and not the real absorbing surface, a detailed post-processing was implemented to determine the heat flux on each panel.

The results obtained with DELSOL3 for the PS10 plant were compared with two types of data available in literature: flux maps [11] and energetic performance indices [10]. The energy flux on the four different panels of the PS10 cavity receiver were created through the Excel[®] interface with four separate runs of the DELSOL3. The flux map obtained on the 21st of March at solar noon assuming as aim point of all the heliostat the center of the aperture showed a vertical off-set with respect to the reference data [11]: the aiming point was therefore lowered by two meters in order to match the maxima real position in the middle of the panels. Fig. 1, left, shows a comparison between the measured solar flux on the panels (top left) and the output of the DELSOL3 software (bottom left). The same comparison was performed on June 21st at 4 pm, as reported in Fig. 1, right.

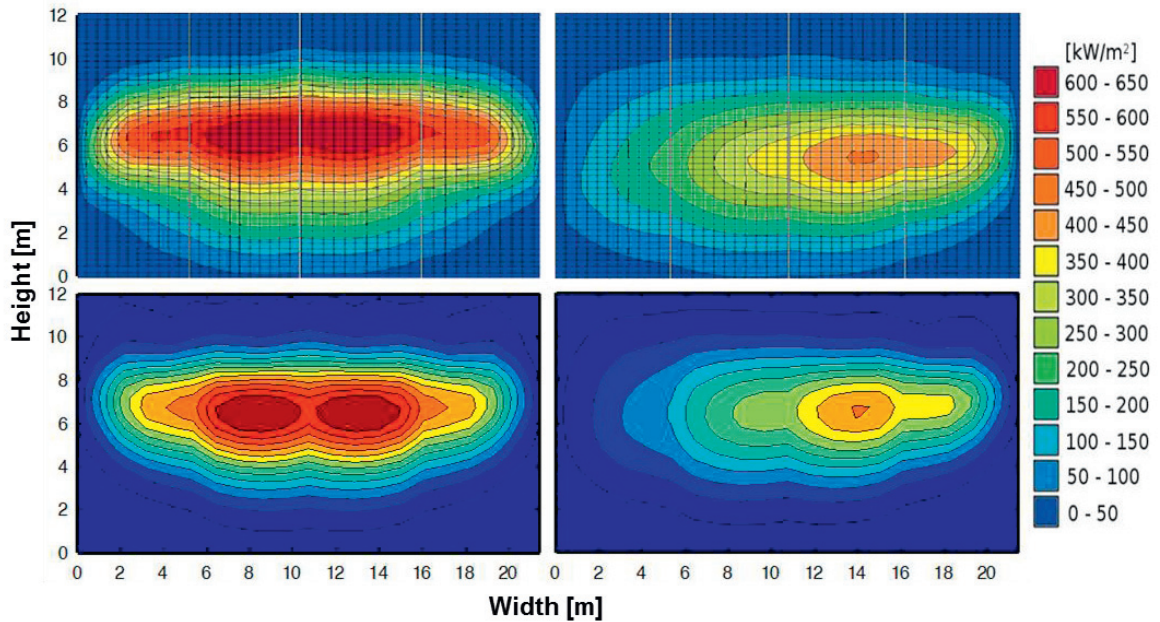


Fig. 1 PS10 flux map on the 21st of March at solar noon (left), and on the 21st of June at 4 pm (right): comparison between data available in literature (top) [11] and DELSOL3 output (bottom);

As shown in Table 3, the peak flux is about 10% higher than experimental data in both days, while there is good accordance in terms of overall concentrated solar radiation. No information was available on the adopted aiming strategy, which significantly influences the values of the peak fluxes: an optimization process could have been considered to reduce this difference, with negligible impact on the optical efficiency; however it was beyond the scope of the work.

Table 3. Numerical results from flux maps: comparison between data and DELSOL3 output.

	March 21 st , noon			June 21 st , 4 pm		
	Model [11]	Simulation DELSOL3	Gap	Model [11]	Simulation DELSOL3	Gap
\dot{Q}_{rec} [MW]	54.7	54.8	0.2%	36.8	36.4	1.1%
Flux Peak [kW/m ²]	650	714	9.8%	455	505	11.0%
$\eta_{optical-DELSOL3}$	0.745	0.746	0.2%	0.603	0.596	1.1%

The software allows also obtaining the optical performance of each heliostat in the simulated field for a selected position of the sun in the sky. An example of total optical efficiency of each mirror is reported in Fig. 2 and Fig. 3 both at solar noon on the summer and winter solstices for the PS10 and the Gemasolar solar fields respectively. The larger dimension of the Gemasolar solar field, with respect to PS10 one, is paid terms of more significant cosine effect and attenuation losses. The heliostats of the PS10 have an efficiency increase in wintertime due to the north oriented solar field layout, while the average performance of the Gemasolar heliostats field has a significant decay for the low solar altitudes occurring during winter. In both fields, it can be noticed the shadow cast on the heliostat closer to the tower northward.

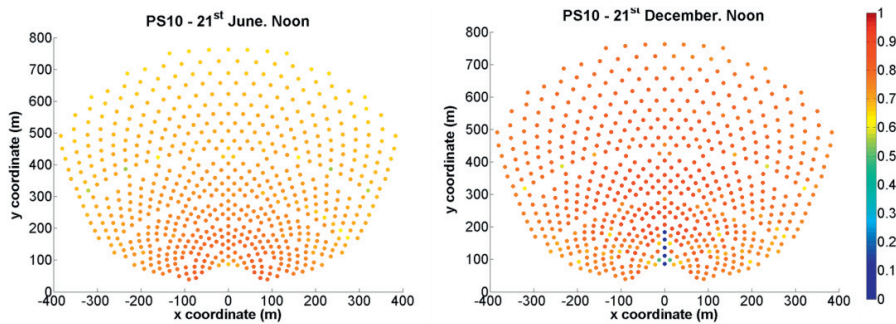


Fig. 2. PS10 heliostats optical efficiencies at solar noon on summer (left) and winter (right) solstices.

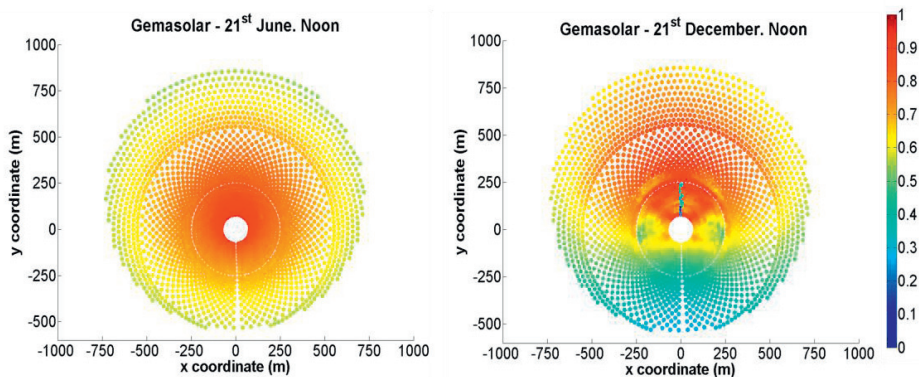


Fig. 3. Gemasolar heliostats optical efficiencies at solar noon on summer (left) and winter (right) solstices.

The software was then used to create the optical efficiency matrixes function of Azimuth and Zenith angle to be used as input in the Thermoflex 23[®] *Solar Tower* component. The sizing on the solar fields in Thermoflex was made on the spring equinox at solar noon varying the design DNI in order to match both the real plants solar field sizes and the solar radiation hitting the receivers [2][10]. The optical efficiency yearly results for the two plants are reported in paragraph 5.

4. Solar plant simulation

The receiver losses include the solar radiation reflected by the receiver (not considered in DELSOL3) and the convective and radiative thermal losses. Thermoflex applies a simplified approach, considering them as a fraction of the solar radiation impinging on the absorber. For the PS10 receiver, Thermoflex model was calibrated at nominal conditions according to [2], while Thermoflex suggested values for molten salts receivers were applied to the Gemasolar cylindrical receiver [4]. In off-design conditions, it was assumed to keep the receiver absorbance constant, as well as the absolute value of the radiative and convective losses.

Power block performance is significantly affected by partial load. Off-design modeling implemented in Thermoflex 23[®] was applied: this takes into account steam-turbine isentropic efficiency variation and realistic pressure conditions at regenerative bleedings at off-design conditions, as well as boiler and feedwater preheater performance [4]. Input defined by the user is the steam-turbine control modality at partial load. Thermoflex 23[®] allows grouping all the different sections of the steam turbine in the so-called steam-turbine assembly, guaranteeing better accuracy in predicting off-design performance.

The power block lay-out implemented in Thermoflex 23[®] for the Gemasolar plant is shown in Fig. 4, while the PS-10 lay-out is the same as in [12]. The boiler section consists of an evaporator, two parallel heat exchangers for

steam superheating and reheating and the economizer. The steam mass flow is set in order to have a turbine power output of 20 MW. The steam expansion is divided in seven groups. The first group, which represents the HP section, is a controlled stage and expands the steam from 100 bar to 42.84 bar. After RH, the steam is expanded down to 0.12 bar at which condensation occurs. In all considered cases, dry condensation is assumed to limit water management issues [13].

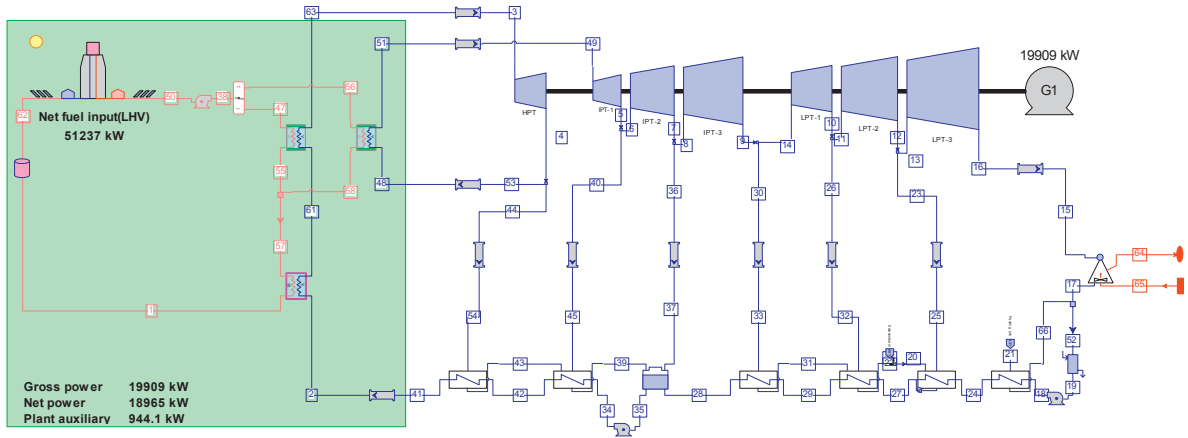


Fig. 4. Gemasolar layout implemented in ThermoFlex 23[®].

Molten salt storage is based on the direct storage concept with two tanks at 270°C and 565°C respectively. The size of the storage is about twice the Andasol case (15 hrs vs. 7.7 hrs), therefore a control strategy which minimizes start-up/shut-down of the steam turbine is implemented. When the hot tank capacity is above 50%, the steam turbine power output is regulated in order to (i) produce a constant power output throughout the night and (ii) empty the hot tank when the solar field starts to work. When the hot tank capacity is below 50%, the storage is emptied up to about 15%, and then the power block is shut-down until the morning. An example of storage/power block control strategy is shown in Fig. 5.

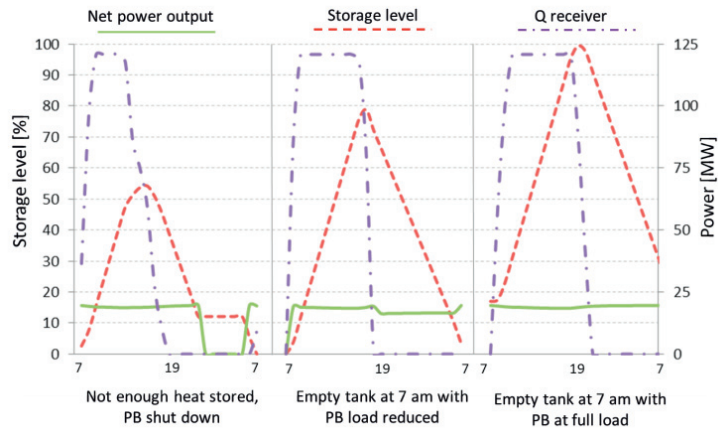


Fig. 5. Power block and TES control strategy in three different days depending on the amount of heat stored.

5. Results

In Fig. 6, the optical ratios (OR) of the selected technologies are shown in order to assist the analysis of the optical performance trend for the different systems during the year. As stated in [14] the OR represents the ratio between the off-design optical efficiency and the optical efficiency at reference condition. For line focusing systems the reference condition is usually with a zero incidence angle so an ideal situation, while for solar tower systems the concept of incidence angle is not useful to identify a reference condition; for this reason, considering the existing differences between PS10 and Gemasolar, the 21st March at solar noon was selected as a reference. It is important to underline that the charts in Fig. 6 which show OR trends during the year give information about the shape of the annual profile but they cannot be used to compare absolute value among different technologies (linear vs. point focus) because of the different reference conditions and nominal optical efficiency. It is worth to notice that solar tower technology has a more constant optical ratio during the year; this characteristic represents an advantage for the operation of the plant compared with PT and LFR which suffer a more variable OR during both day and year.

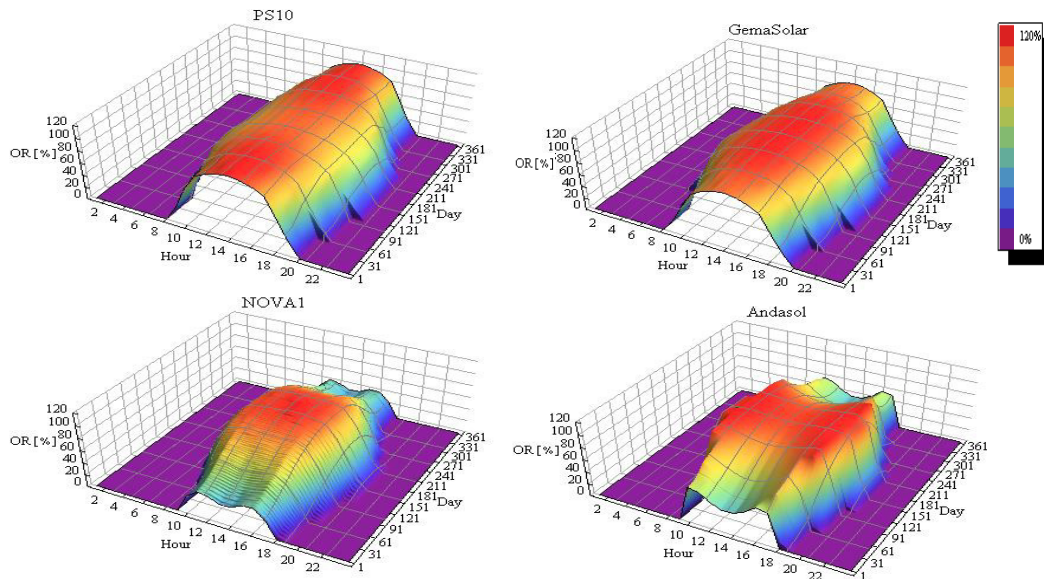


Fig. 6. Optical Ratios (OR) for the four different considered plants as a function of the hour of the day and of the day of the year.

Table 4 summarizes all the terms in which optical efficiency of solar tower is split, including also the absorbance contribution ($\eta_{\text{absorbance}}$) not taken into account in DELSOL3. As previously underlined, the main differences in the two solar tower systems are the orientation of the solar field and the occupied area that lead to different behavior in the optical efficiency components.

Referring to nominal efficiency (21st March at solar noon) it is possible to notice the relevant difference in the “cosine effect” term. PS10 has a higher value of η_{cos} because of both the smaller occupied area (equivalent to a lower mean distance mirror-receiver) and the different orientation of the solar field. North field takes advantage of the solar position in reference condition compared with the circular field of Gemasolar. As regards Gemasolar plant, the higher mean distance between mirrors and receiver explains the bigger value of spillage and atmospheric attenuation while the assumed higher mirror reflectivity (93% vs 88% as in Table 1) partly balances the abovementioned penalties.

In order to avoid heavy off-design condition the maximum power is limited with the implementation of defocusing which is described by the parameter η_{defocus} (%). It is possible to notice how Gemasolar defocuses mirrors more frequently than PS10. This fact is related to the sizing characteristics of the two plants; in particular

during days of high radiation can occur that Gemasolar will be unable to use all the thermal energy in the storage and in the next day thermal storage can reach the maximum level which determines the condition of starting defocus. However, the oversize of solar field in Gemasolar guarantees a significant power production also in winter. In PS10 the sizing, characterized by the presence of a small thermal storage (steam buffer), leads to defocus only when the maximum electric power of the turbine is reached.

Table 4. PS10 and Gemasolar nominal and annual optical efficiency, split into different contributions.

	PS10		Gemasolar	
	Nominal	Annual	Nominal	Annual
η_{\cos} (%)	92.34	84.40	81.44	76.62
η_{reflect} (%)	88.00	88.00	93.00	93.00
η_{shadow} (%)	99.93	96.56	99.83	94.84
η_{block} (%)	99.24	99.09	99.63	98.44
$\eta_{\text{attenuation}}$ (%)	95.44	95.50	95.04	95.03
η_{spillage} (%)	99.34	99.39	95.53	95.08
$\eta_{\text{absorbance}}$ (%)	98.00	98.00	97.00	97.00
η_{optical} (%)	74.87	66.10	66.34	58.31
η_{defocus} (%)		97.90		86.47

The “chain of five efficiencies” [6] [7] for each considered plant and the resulting overall efficiency are reported in Table 5. Comparing the solar tower cases (PS10 and Gemasolar), the penalty for a lower optical efficiency of Gemasolar, which includes also the defocus effect, is overtaken by the advantage of a higher power block efficiency leading to a higher overall nominal efficiency. In addition to the thermodynamic advantage of power block previously underlined, Gemasolar, in comparison with PS10, benefits of the presence of the thermal storage that allows more stable working conditions reducing off-design operation penalizations.

Table 5. Efficiencies comparison among the selected plants

	PS10	Gemasolar	PE-1	Andasol I
$\eta_{\text{optical nominal}}$ (%)	74.87	66.34	63.65	76.00
$\eta_{\text{overall nominal}}$ (%)	19.55	23.62	18.07	22.09
$\eta_{\text{optical yearly}}$ (%)	64.72	50.42	39.65	55.96
$\eta_{\text{thermal yearly}}$ (%)	92.83	94.47	90.68	92.11
$\eta_{\text{piping yearly}}$ (%)	98.85	99.87	99.68	97.9
$\eta_{\text{net PB yearly}}$ (%)	27.33	39.07	29.23	35.77
$\eta_{\text{aux SF yearly}}$ (%)	98.85	98.69	99.52	95.6
$\eta_{\text{overall yearly}}$ (%)	16.05	18.34	10.43	15.41

The comparison between the two linear focus technologies, investigated in detailed in [14], highlights that the higher performances of parabolic trough mainly derived from a higher annual optical efficiency and a higher power block performance. Choosing the best representative of the two concentrating technologies, the last comparison is between the Gemasolar plant and the Andasol plant that nowadays represents the commercial technologies.

The higher overall energy performance of Gemasolar is mainly explained by:

- Higher thermal efficiency related to the higher concentration ratio of solar tower;
- Higher power block efficiency related to higher maximum temperature of the thermodynamic cycle;
- Lower impact of SF auxiliaries: parabolic trough need a pump to circulate the fluid in the solar field that represents the most important auxiliary consumption;
- Reduced piping systems compared to the parabolic trough plant implies lower thermal losses.

Limiting the comparison to energetic analysis among commercial CSP solution, solar tower plant with the characteristic of Gemasolar represents a good alternative to parabolic trough like Andasol. It is important to underline that more complete evaluation needs to consider economic aspects related to the cost of electricity and a detailed economic analysis will be the topic of future works.

6. Conclusions

This work aimed at comparing two commercial Concentrated Solar Power plants in terms of annual performances, therefore assuming different operating conditions and set of assumptions (e.g. the heliostats reflectivity for the two solar tower plants). For this purpose, two different tools were adopted and calibrated towards available data: DELSOL3 was used for the optical assessment, and its results were used as input to Thermoflex 23[®] which models the entire systems.

The optical assessment showed that in Seville the surrounded field has lower yearly performances than the north configuration because of the cosine effect. Moreover, the conversion efficiency from thermal energy to electricity is the most important part of the conversion process: the optical efficiency can vary in relative terms of about 20-25%, while the power block efficiency variation can be as high as 50%. Finally, the point focus systems have little efficiency advantages compared to parabolic trough technologies, while significant compared to Linear Fresnel Collectors. A step further which will be discussed in a future work is the comparison in terms of investment costs and cost of electricity, as well as a plant optimization from economic point of view.

References

- [1] A.Meier, C.Sattler. *Solar fuels from concentrated sunlight*. Solar Power and Chemical Energy Systems Implementing Agreement of the International Energy Agency. s.l. : SolarPACES, August 2009, 2009.
- [2] SENER. Case Study: GEMASOLAR Central Tower Plant. [Online] 2010. www.sener.es.
- [3] Solúcar. *10 MW Solar Thermal Power Plant for Southern Spain*. 2006. NNE5-1999-356.
- [4] Thermoflow. *Thermoflex Help System*. 2010.
- [5] Kistler, Bruce L. *A User's Manual for DELSOL3: A Computer Code for Calculating the Optical Performance and Optimal System Design for Solar Thermal Central Receiver Plants*. 1986.
- [6] G. Manzolini, A. Giostri, C. Saccilotto, P. Silva, E. Macchi. Development of an innovative code for the design of thermodynamic solar power plants Part A: Code description and test case. *Renewable Energy*. July 2011, Vol. 6, p. 1993-2003. doi:10.1016/j.renene.2010.12.027.
- [7] —. Development of an innovative code for the design of thermodynamic solar power plants Part B: Performance assessment of commercial and innovative technologies. *Renewable Energy*. 2011, In Press. doi:10.1016/j.renene.2011.02.003.
- [8] A.Giostri, M.Binotti, M.Astolfi, P.Silva, E.Macchi, G.Manzolini. Comparison of different solar plants based on parabolic trough technology. *Solar Energy*. Vol. 86, 5, p. 1208-1221.
- [9] *Gemasolar, key points for the operation of the plant*. Burgaleta, Juan Ignacio, et al. 2012. Proceedings of the 18th SolarPACES International Conference.
- [10] Fernández, Valerio D. PS10: a 11.0-MWe Solar Tower Power Plant with Saturated Steam Receiver. [Online] 2005. <http://www.upcomillas.es/catedras/crm/report05/Comunicaciones/Mesa%20IV/D.%20Valerio%20Fern%20C3%A1ndez%20-%20Solucar%202.pdf>
- [11] Osuna, Rafael. Solar thermal industry, success stories and perspectives. [Online] <http://ec.europa.eu>.
- [12] Colzi, Filippo e Petrucci, Stefano. *Modeling On/Off - Design performance of solar tower plants*. s.l. : Politecnico di Milano, AA 2008 - 2009.
- [13] Turchi CS, Wagner MJ, KutscherCF. Water Use in parabolic trough power plants: summary results. *Worley parsons analysis*.
- [14] A.Giostri, M.Binotti, P.Silva, E.Macchi, G.Manzolini. Comparison of Two Linear Collectors in Solar Thermal Plants - Parabolic Trough Versus Fresnel. *Journal of Solar Energy Engineering*. 2013, Vol. 135, 1.